JOURNAL OF MATERIALS SCIENCE 20 (1985) 1291–1300

# The hydrogen reduction of cobalt–tungsten mixed oxides

G. J. FRENCH*, F. R. SALE
*Department of Metallurgy and Materials Science, University of Manchester, Grosvenor Street, Manchester, UK*

The hydrogen reduction of two non-stoichiometric samples of cobalt tungstate (one cobalt-rich, the other heavily tungsten-rich) has been studied over the temperature range 600 to 1100° C using thermogravimetry, X-ray diffraction analysis and scanning electron microscopy. The products are shown to be non-equilibrium at most reduction temperatures. In order to explain the experimentally observed X-ray diffraction data it is postulated that the reduction process occurs via the formation of an amorphous phase which contains cobalt, tungsten and oxygen. The amorphous phase becomes unstable at low oxygen potentials and precipitates either, or both, $Co_3W$ and $Co_7W_6$ depending upon the degree of cobalt enrichment of the amorphous phase. These are the only two cobalt-containing crystalline phases in the products of reduction and are not detected before at least 53% reduction has occurred. During the early stages of reduction either tungsten (for near stoichiometric, cobalt-rich oxide) or $WO_2$ (for tungsten-rich oxide – $CoWO_4$ plus $WO_3$) are the only crystalline products of reduction.

## 1. Introduction

Over recent years a number of workers have considered the carburization of mixed cobalt and tungsten oxides for the direct production of tungsten carbide–cobalt composite material [1–3]. Industrially, Gortsema and Kotval [1] have studied the reduction/carburization of "precursor-derived" mixtures of $CoWO_4$ and $WO_3$ using $CO/CO_2$ and $H_2/CH_4$ and Takatsu [2] has studied the reduction/carburization of $CoWO_4$ and $WO_3$ mixtures in a rotary kiln using $H_2/CH_4$. Ushijima [3] prepared Co/WC powders by the direct carburization of $WO_3$ and $Co_3O_4$ with carbon black. Thermodynamic predictions on the reduction/carburization of $CoWO_4$ have shown that certain advantages, notably a potentially greater control of free carbon content, should be available with the use of $H_2/CH_4$ gas mixtures rather than $CO/CO_2$ mixtures [4]. Accordingly, a study of the controlled reduction/carburization of $CoWO_4$ in $H_2/CH_4$ mixtures has been carried out by the present authors [5]. During the early stages of this study it was determined that the mechanism of reduction/carburization was such that complete reduction of the tungstate to a metallic phase occurred before any carburization began. Consequently, a study of the hydrogen reduction of two commercial samples of cobalt tungstate has been carried out in order to obtain information relevant to the first stage of reduction/carburization in $H_2/CH_4$ mixtures.

In his study of the reduction behaviour of metal tungstates, Guerassimov [6] showed that two extreme types of behaviour existed. For metals with high affinities for oxygen, reduction of the metal tungstate led to a dispersion of the metal oxide in tungsten according to:

$$MWO_4(s) + 3H_2(g) \rightarrow MO(s) + W(s) + 3H_2O(g).$$

For metals with a low affinity for oxygen, and which are immiscible with tungsten, reduction of the tungstate yielded a mixture of metal and tungsten, or on partial reduction produced a mixture of the metal and one of the tungsten

---

*Present address: Chloride Technical Ltd, Wynne Avenue, Swinton, Manchester, UK.

0022–2461/85 $03.00 + .12

oxides, depending upon the effective oxygen potential in the system:

$$MWO_4(s) + (4 - x)H_2(g) \rightarrow M(s) + WO_x(s) + (4 - x)H_2O(g)$$

where $2 < x < 3$. This latter type of reduction behaviour has been investigated more fully for copper tungstate [7, 8] and silver tungstate [9, 10] for the production of composite powder mixtures for applications in the electrical contact industry.

Tungstates of iron, nickel and cobalt were predicted by Guerassimov [6] to have intermediate reduction behaviour and to yield mixtures of tungsten alloys, intermetallic compounds, tungsten metal and/or tungsten oxides. Bracconi and Dufour [11, 12] have investigated the reduction of stoichiometric $CoWO_4$ over the temperature range 425 to 1000° C and have identified an intermediate ternary phase during reduction. Phase relationships in the dioxide–trioxide regions of some 3d transition metal–W–O systems have also been reported by Ekstrom and Tilley [13] who did not detect any ternary phases other than $CoWO_4$ in the Co–W–O system. The systems Mn–W–O and Fe–W–O, however, were found to contain ternary compounds other than the tungstates, whereas the system Ni–W–O was shown to be similar to that for Co–W–O. Consequently, it was anticipated that the present study would provide data for comparison with the results of these other workers [6, 11–13] as well as allowing identification of the products of the first stage of reduction/carburization of the commercial cobalt tungstate samples for the production of Co/WC mixtures.

## 2. Experimental procedure

### 2.1. Materials

Two samples of cobalt–tungsten oxides of differing particle morphology and composition were studied. The first sample was purchased from Cerac/Pure Inc, and henceforth will be identified as "Cerac" material. Although supplied as pure stoichiometric cobalt tungstate ($CoWO_4$) with a maximum impurity limit of 0.05 wt%, the sample was found to be cobalt-rich by atomic absorption analysis and had a composition which could be expressed as $4CoWO_4 \cdot 2CoO$. This powder was used in the as-received state in the hydrogen reduction experiments.

The second sample was supplied by Murex Ltd, and had been prepared using a precipitation technique which involved the mixing of solutions of ammonium paratungstate and cobalt sulphate. The resulting precipitate was filtered, washed and dried at 60° C in air. The solutions were mixed in proportions to give $3CoWO_4 \cdot 4WO_3 \cdot 25H_2O$, however, the solution remaining after precipitation was shown to contain cobalt. Before reduction, the powder was dehydrated by heating at 300° C in air for 6 h. Chemical analysis of the dehydrated sample gave a composition $3CoWO_4 \cdot 5WO_3$.

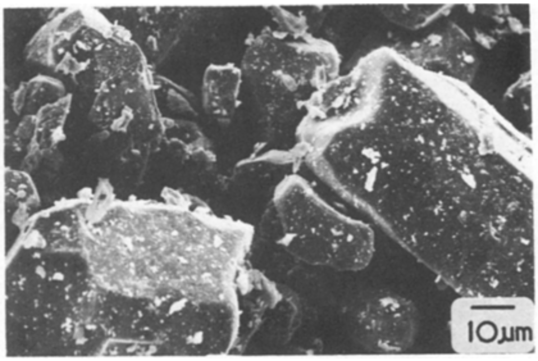

*Figure 1* Scanning electron micrograph of as-received "Cerac" cobalt tungstate.

Both oxide samples were studied in a "Philips 505" scanning electron microscope to determine their particle sizes and morphologies before reduction. Figs. 1 and 2 show representative micrographs of these oxides.

### 2.2. Reduction studies

A "C.I. Electronics 2CT5" electromagnetic balance was used in conjunction with a "Nichrome" wound furnace, which was controlled by a "Newtronics" temperature controller, to study the reduction of the oxide samples. The furnace was movable and so allowed the reduction of a given

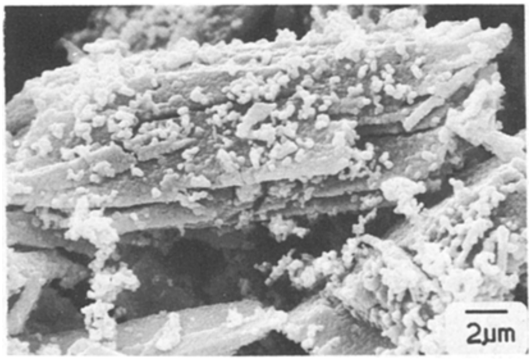

*Figure 2* Scanning electron micrograph of "Murex" cobalt tungstate after calcination at 300° C.

sample to be arrested at any point in time and also allowed easy retrieval of partially and fully reduced samples for characterization by X-ray diffraction analysis and scanning electron microscopy. Before and after reduction the balance was flushed with nitrogen.

Samples of both oxide mixtures were reduced at temperatures between 600 and 1100° C. For each oxide, a complete series of reductions, interrupted at intervals of 10% of expected maximum weight loss was carried out at 800° C.

### 2.3. Characterization of materials

X-ray diffraction analysis of the products of partial and full reduction was carried out with a "Philips" horizontal diffractometer scanning over the range 15° to 90° at a rate of 6° min$^{-1}$ using Cu$K\alpha$ radiation. The same samples of reduction products were also studied on the "Philips 505" scanning electron microscope to determine whether significant morphological changes occurred during reduction. Analysis of some of the powder samples was carried out using an EDAX energy dispersive X-ray analyser attached to the scanning electron microscope.

## 3. Results

### 3.1. Thermogravimetric measurements

The results of the thermogravimetric studies of the reduction processes, expressed as the relationship between percentage weight loss and time, are shown in Figs. 3 and 4 for the "Cerac" material and in Figs. 5 and 6 for the "Murex" material. From Figs. 3 and 4 it is evident that at all temperatures studied the reduction occurred continuously in what appears to be a single-stage process, without any marked decreases and increases in rate as time progressed, such that smooth curves of weight loss as a function of time resulted. However, increases in temperature produced marked decreases in time required for complete reduction; at 800° C the reduction time was only 20% of that required at 700° C.

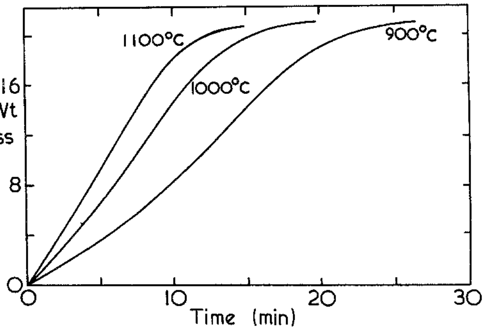

*Figure 4* Relationship between % weight loss and time for reduction of "Cerac" material at 900, 1000 and 1100° C.

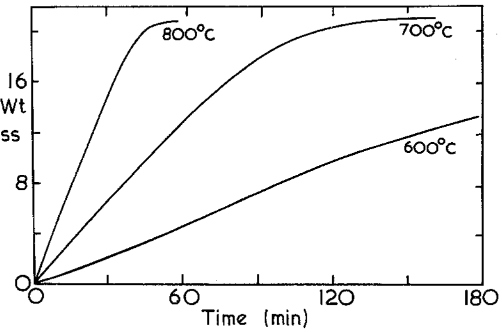

*Figure 3* Relationship between % weight loss and time for reduction of "Cerac" material at 600, 700 and 800° C.

It can be seen from Figs. 5 and 6 that at temperatures between 600 and 900° C the reduction of the "Murex" material is unlike that of the "Cerac" material. Over this temperature range a multi-stage reduction sequence is evident from the thermogravimetric data for the "Murex" material. At higher temperatures it can be seen that either the successive stages overlap such that a smooth reduction curve is obtained or a single-stage process occurs. At reduction temperatures of 600 and 700° C two definite inflexions can be identified in the weight loss curves. The first inflexion occurs at 3.8% weight loss and is accompanied by a marked decrease in reduction rate. The second inflexion is less noticeable and occurs at 14% weight loss. After the second inflexion the weight loss curves are smooth up to the final weight loss of approximately 20.8%.

### 3.2. X-ray diffraction analysis

The results of the X-ray diffraction analyses of the

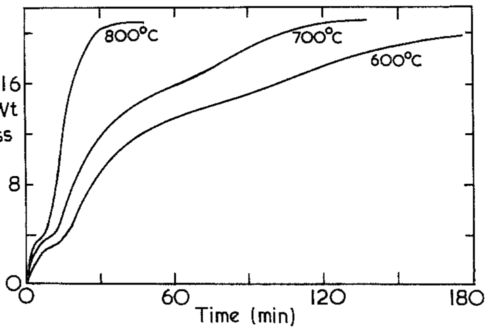

*Figure 5* Relationship between % weight loss and time for reduction of calcined "Murex" material at 600, 700 and 800° C.

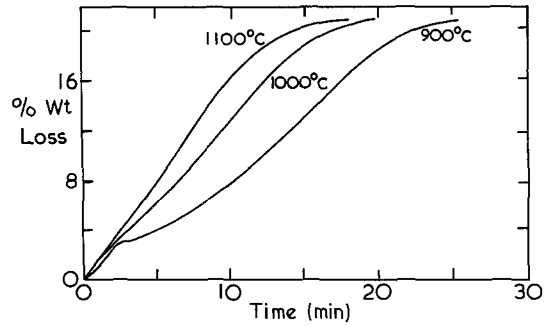

*Figure 6* Relationship between % weight loss and time for reduction of calcined "Murex" material at 900, 1000 and 1100° C.

various reduction products are summarized graphically in Figs. 7 and 8 for the "Cerac" material and in Figs. 9 and 10 for the "Murex" material. In these figures the experimental data are shown as the relative intensities of the 100% diffraction peak of the phases identified (taken as the fraction of the summed total of the 100% intensity lines for each phase identified) plotted as a function of the reduction temperature (Figs. 7 and 9) and as a function of the percentage reduction at 800° C (Figs. 8 and 10). This presentation of the data is qualitative as it does not take into full account either the quantities of phases or their specific X-ray diffraction nature. However, such a representation gives a clear indication of the relative changes in the phases identified as a function of temperature and time of reduction.

From Fig. 7 it can be seen that the predominant products of reduction of the "Cerac" material at 600 and 700° C are $\beta$-tungsten and the intermetallic compound $Co_3W$. Traces of $\alpha$-tungsten and the compound $Co_7W_6$ were also detected in the products obtained at 700° C. At 800° C the $\beta$-tungsten has been replaced completely by $\alpha$-tungsten and by 900° C the $Co_3W$ has disappeared completely leaving only $Co_7W_6$ and $\alpha$-tungsten as the products of reduction. Above 900° C there is an increase in the $Co_7W_6$ as a corresponding decrease in $\alpha$-tungsten occurs. It is apparent from Fig. 8 that reduction of the "Cerac" material at 800° C leads to a progressive disappearance of $CoWO_4$ which yields initially (up to 53% reduction) $\alpha$-tungsten as the only product identifiable by X-ray diffraction. $Co_3W$ is detected as the first cobalt-containing phase and $Co_7W_6$ appears at approximately 85% reduction. $CoWO_4$ becomes undetectable at 90% reduction.

It is evident from Fig. 9 that the "Murex" material gives products of reduction of $\beta$- and $\alpha$-tungsten, and $Co_3W$ at 600° C. However, at higher reduction temperatures the $\beta$-tungsten and $Co_3W$ levels decrease with commensurate increases in the amounts of $\alpha$-tungsten and $Co_7W_6$. The $\beta$-tungsten and $Co_3W$ have both disappeared from the products of complete reduction by 800° C. From the data obtained during the progress of the reduction reaction, which is shown in Fig. 10, it is evident that there is a rapid decrease in the $WO_3$ content of the oxide mixture. This decrease is accompanied by an increase in the $WO_2$ level. The final disappearance of $WO_3$ by 15% reduction corresponds to a weight loss of 3.8%. Thus it can be seen that the first inflexion on the thermogravimetric curve for the "Murex" oxide corresponds to the decrease in reduction rate which occurs once all the $WO_3$ has been converted to $WO_2$. After the disappearance of the $WO_3$, the $WO_2$ level continues to increase as the $CoWO_4$ level decreases and eventually becomes undetectable at approximately 65% reduction. At this point in the reduction sequence the $WO_2$ level begins to decrease as the level of $\alpha$-tungsten increases. The disappearance of $CoWO_4$ from the product corresponds to the second inflexion seen on the thermogravimetric curves for this sample. Above 70% reduction $Co_7W_6$ appears as reduction product.

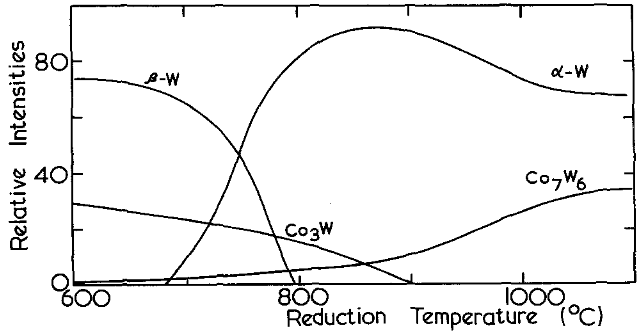

*Figure 7* Variation of relative intensities of product phases as a function of reduction temperature for "Cerac" material.

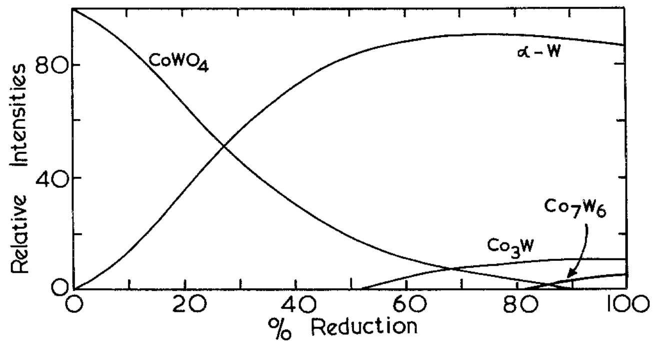

*Figure 8* Variation of relative intensities of phases identified as a function of % reduction at 800° C for "Cerac" material.

### 3.3. Product morphologies

The morphologies of the products obtained on reduction of the "Cerac" material at temperatures of 700, 900 and 1100° C are shown in Figs. 11, 12 and 13, respectively. It can be seen that reduction at low temperatures (700 and 600° C) leaves the material virtually unaltered with the product being obtained as a pseudo-morph of the original oxide. The only slight morphological change is the small amount of surface roughening which occurs as a result of reduction. At higher reduction temperatures (800 and 900° C), as shown in Fig. 12, a considerable amount of surface recrystallization occurs and this results in the formation of the discrete crystallites which can be seen on the surface of the original oxide particles. EDAX analysis of the recrystallized surface has shown it to be tungsten-rich (68.44 at% tungsten, 31.56 at% cobalt), which is unexpected as the overall composition of the material is cobalt-rich. This observation indicates that the production of tungsten as the first product of reduction must occur on the surfaces of the original oxide particles with a corresponding increase in the cobalt level of the interior of the original particles. At the higher reduction temperatures of 1000 and 1100° C the degree of breakdown of the original oxide is more extensive and the individual crystallites are larger and more sintered than those obtained at 800 and 900° C. Fig. 13 shows the interior of one of the agglomerates of recrystallized particles and it can be seen that a mixture of acicular "needles" or "stringers", measuring up to 15 μm in length, exists along with large rounded particles beneath the surface layer of partially sintered crystallites.

The products obtained by reduction of the "Murex" oxide material at 700, 900 and 1100° C are shown in Figs. 14, 15 and 16, respectively. In contrast to the "Cerac" material surface crystallites can be seen to form at low temperatures (Fig. 14). The trend of increasing surface crystallite size with reduction temperature, which was seen for the "Cerac" material, can also be seen to exist for the "Murex" oxide (Figs. 15 and 16). At 1100° C a greater degree of sintering and faceting can be seen for the products from the "Murex" material relative to the "Cerac" material.

## 4. Discussion

### 4.1. Reduction mechanism for "Cerac" material

The theoretical reduction routes for both the "Cerac" and "Murex" oxide are shown in Fig. 17 which gives the isothermal section for the Co–W–O phase diagram at 1000° C. This section may be taken as representative of the Co–W–O system

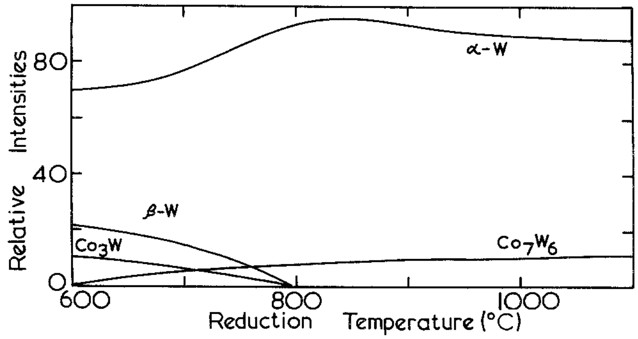

*Figure 9* Variations of relative intensities of products phases as a function of reduction temperature for calcined "Murex" material.

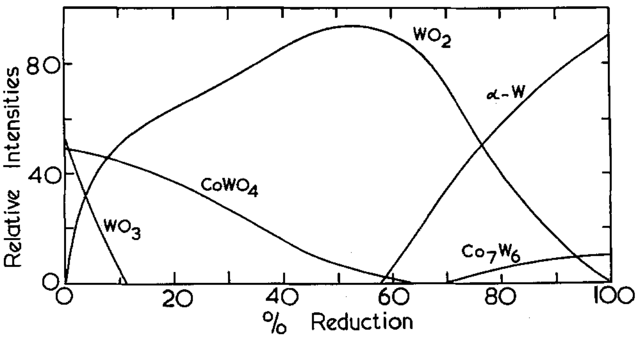

*Figure 10* Variation of relative intensities of phases identified as a function of % reduction at 800° C for calcined "Murex" material.

over the temperature range investigated in this study. According to Fig. 17 the final equilibrium product of reduction of "Cerac" oxide should be a mixture of $Co_7W_6$ and $Co_3W$. Consequently, the appearance of $\beta$- and $\alpha$-tungsten in the reduction products indicates the non-equilibrium nature of the reduction process over the temperature range studied. The X-ray diffraction analyses of the products obtained at various times and temperatures of reduction did not detect any cobalt-containing phase (other than residual $CoWO_4$) until greater than 50% reduction had occurred. However, as either $\beta$- or $\alpha$-tungsten were detected in the products after very short reduction periods, along with a commensurate decrease in the amount of $CoWO_4$ present, it appears that cobalt is either retained in a non-crystalline amorphous phase or it is dispersed in such a fine particulate form that it does not produce a diffraction pattern. As metallic cobalt was never detected in the reduction products the former suggestion seems more likely.

Cobalt tungstate ($CoWO_4$) has a distorted hexagonal crystal structure whilst $Co_7W_6$ has a complex rhombohedral $D^8_5$ crystal structure and $Co_3W$ has a complex hexagonal $D^0_{19}$ structure. Consequently, the formation of either of the two intermetallic compounds from the tungstate is difficult and requires a large amount of atomic rearrangement concomitant with the removal of oxygen from the tungstate. As a result, it appears that the precipitation of either $\alpha$- or $\beta$-tungsten (depending upon the prevailing oxygen potential) is a kinetically favoured step during reduction along with the production of a cobalt-enriched ternary amorphous phase. The amorphous phase appears to be stabilized by the presence of oxygen and the degree of cobalt enrichment that occurs is dependent upon the time and temperature of reduction. In addition, it appears that once a critical oxygen level is achieved in the amorphous phase it becomes unstable and results in the precipitation of intermetallic compounds. Accordingly, at 600° C when reduction is very slow, large amounts of oxygen-stabilized $\beta$-tungsten are precipitated and the amorphous phase is enriched to a composition close to $Co_3W$ such that once the oxygen level has been decreased by hydrogen reduction beyond the critical value the intermetallic compound $Co_3W$ is produced. At higher

*Figure 11* Scanning electron micrograph of product ol reduction of "Cerac" cobalt tungstate at 700° C.

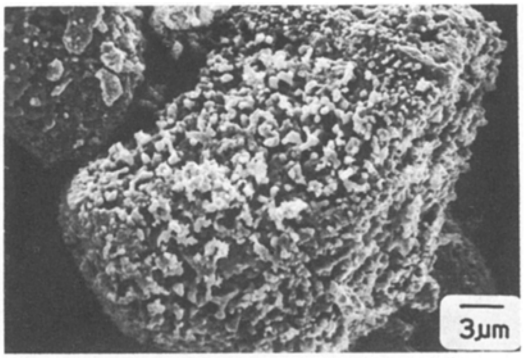

*Figure 12* Scanning electron micrograph of product of reduction of "Cerac" cobalt tungstate at 900° C.

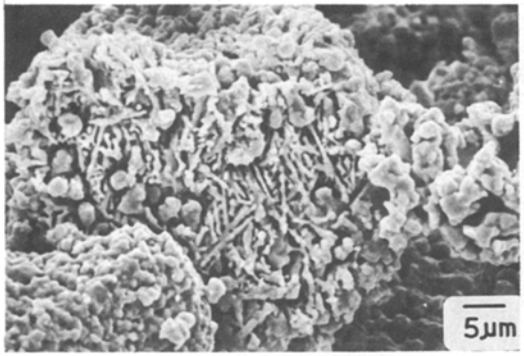

*Figure 13* Scanning electron micrograph of product of reduction of "Cerac" cobalt tungstate at 1100° C.

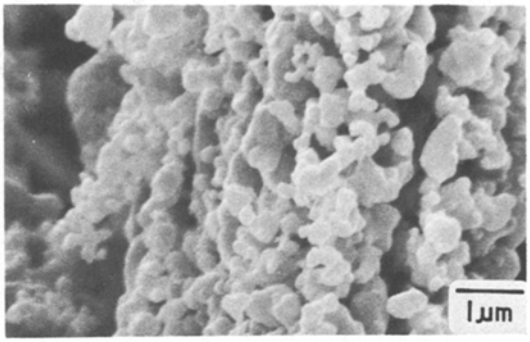

*Figure 15* Scanning electron micrograph of product of reduction of calcined "Murex" material at 900° C.

reduction temperatures, where the removal of oxygen occurs more rapidly, a smaller cobalt enrichment occurs as a result of less tungsten production. At temperatures up to 900° C it appears that $Co_3W$ is still produced as the first intermetallic compound, however, because of a lower level of cobalt enrichment of the ternary phase, the precipitation of $Co_3W$ reduces the cobalt content of the ternary phase to a point where $Co_7W_6$ is eventually precipitated. At higher temperatures it seems that the cobalt-enrichment does not occur past the composition required for $Co_7W_6$ production. Consequently, on achieving the critically low oxygen content $Co_7W_6$ is produced leaving α-tungsten and $Co_7W_6$ as the sole products of high-temperature reduction.

The postulation of the ternary amorphous phase, which becomes cobalt-enriched as tungsten precipitation occurs, is in broad agreement with the experimental results and discussion of Bracconi and Dufour [11, 12]. In their investigation of the reduction of stoichiometric $CoWO_4$ over the temperature range 425 to 1000° C, X-ray diffraction analyses of products at 550° C showed the progressive disappearance of $CoWO_4$ with the appearance of what was described as an intermediate, unstable phase and a single final product phase. Structural data for the intermediate phase (denoted $CoW_{1-x}O_y$) was found to be similar to that given for $Co_3W_3O$, the ternary phase proposed by Schonberg [14]. Reduction in $H_2/H_2O$ gas mixtures by Bracconi and Dufour [12] gave data which was interpreted as giving the formula of the phase $CoW_{1-x}O_y$ as $Co_4W_{2.5}O$. According to Bracconi and Dufour this intermediate ternary oxide was reduced further to yield a metallic amorphous phase (designated $\phi$, $CoW_{0.33}$), which contained all the initial cobalt of the tungstate, and, eventually, at temperatures above 425° C, the metallic amorphous phase gave the intermetallic compound $Co_3W$ and $Co_7W_6$ in amounts which varied with the reduction temperature and time. At temperatures above 800° C, $Co_7W_6$ alone was produced as the intermetallic phase. It is, however, difficult to explain the precipitation of both

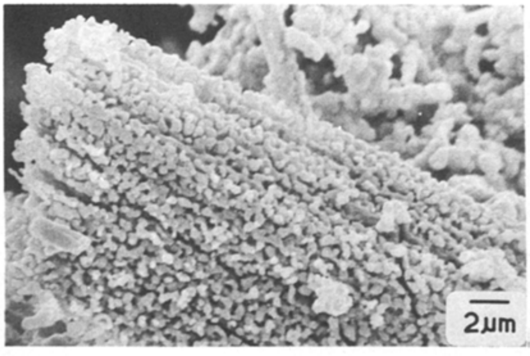

*Figure 14* Scanning electron micrograph of product of reduction of calcined "Murex" material at 700° C.

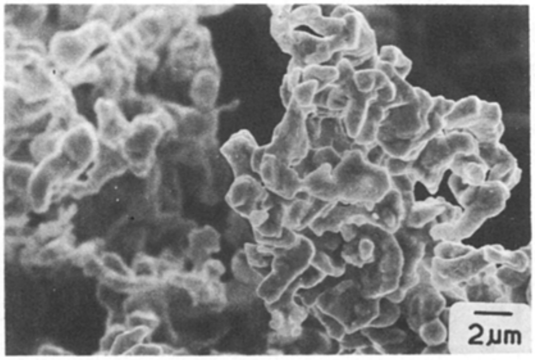

*Figure 16* Scanning electron micrograph of product of reduction of calcined "Murex" material at 1100° C.

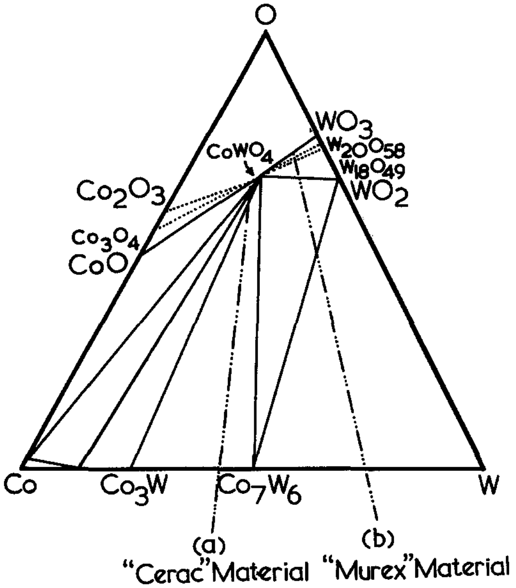

*Figure 17* Isothermal section of the Co–W–O phase diagram at 1000° C showing theoretical reduction routes for materials studied.

intermetallic compounds from a metallic phase of composition $CoW_{0.33}$. In the present study no experimental evidence was found, at any reduction time and temperature, for the ternary crystalline oxide phase which is in agreement with the results of Ekstrom and Tilley [13]. However, as described earlier, it is necessary to invoke the concept of an amorphous cobalt-containing phase in order to explain the experimental X-ray diffraction data. The major difference between the amorphous phase postulated in the present study is that it contains cobalt, tungsten and oxygen, and that it varies in composition, becoming cobalt-enriched, as reduction proceeds. Also it is suggested that the ternary amorphous phase becomes unstable once a critically low oxygen level has been reached. In the work of Bracconi and Dufour [11], reduction at 425° C was shown to yield β-tungsten as the only phase detected by X-ray diffraction analysis. The present authors believe that this low-temperature reduction was incomplete such that the amorphous cobalt-containing phase remained stabilized by oxygen.

## 4.2. Reduction mechanism for "Murex" material

According to Fig. 17 the equilibrium reduction products for the "Murex" oxide should be a mixture of $Co_7W_6$ and α-tungsten. The appearance of $Co_3W$ in the reduction products obtained at low reduction temperatures indicates the non-equilibrium nature of reduction of this oxide, as seen for the "Cerac" material. However, the reduction sequence seen for the "Murex" oxide is quite different to that observed for the "Cerac" material, as a result of the difference in composition of the two samples. The first main stage of reduction of the "Murex" material is the production of $WO_2$ (probably via $W_{20}O_{58}$ and $W_{18}O_{49}$) from the excess $WO_3$ present in the sample. Once $WO_2$ has been produced and all the $WO_3$ has disappeared, reduction of the $CoWO_4$ accelerates. As for the "Cerac" material no crystalline cobalt-containing phase can be detected by X-ray diffraction analysis until the later stages of reduction are reached (70% at 800° C). The main difference between the behaviour of the "Cerac" and "Murex" samples occurs as the $CoWO_4$ is reduced. Whereas for "Cerac" material either β- or α-tungsten was produced as reduction proceeded and the cobalt content of the amorphous phase increased, for the "Murex" sample is appears that $WO_2$ is produced from the $CoWO_4$ as the cobalt content of the amorphous phase is increased. Two possible reasons exist for this behaviour. As $WO_2$ already is present in the products from the $WO_3$ it could be kinetically easier for $WO_2$ to grow on the pre-existing $WO_2$ particles. Alternatively, whilst $WO_2$ is present in the reaction product the effective oxygen potential of the product will be maintained at a level higher than that for β- (or α-tungsten) as reduction of the tungstate occurs, hence more $WO_2$ is produced. From the X-ray diffraction data it is apparent that all the tungstate is reduced (i.e. $CoWO_4$ disappears completely) before any crystalline cobalt-containing product phase can be detected. An explanation for this observation is that the amorphous ternary phase is stabilized by the presence of $WO_2$ in the mixed product because of the high oxygen potential. The implication of this observation is that the critical oxygen potential, below which the amorphous phase becomes unstable and precipitates either $Co_3W$ or $Co_7W_6$, must be below the equilibrium oxygen potential for $WO_2$ at the reduction temperature in question. Tungsten and either $Co_3W$ or $Co_7W_6$ are only detected once the level of $WO_2$ in the partially reduced products begins to decrease (Fig. 10). As for the "Cerac" material, at low temperatures $Co_3W$ and $Co_7W_6$ are obtained in the final product of reduction. However, at higher temperatures $Co_7W_6$ is the only intermetallic compound detected in the reduction products.

The production of β-tungsten from both types of starting material at temperatures greater than 600° C lends credance to the postulation of Morcom *et al.* [15] that the presence of certain metallic elements helps to stabilize β-tungsten above its usual decomposition temperature.

### 4.3. Morphological considerations

As with most processes involving the hydrogen reduction of oxides appreciable particle breakdown and change in particle morphology can be seen to occur at temperatures in excess of 600° C for both oxide samples studied. As for the reduction of other tungsten oxides [7, 9, 16, 17] surface roughening is followed by the formation of discrete crystallites, which are submicron in size, for both samples studied. At the higher temperatures of 1000 and 1100° C, the product powders show evidence of sintering. Consequently, it is apparent that in order to obtain the minimum particle size and maximum surface area for subsequent carburization (as indicated in the Section 1) it is preferable to carry out the reduction at 800 to 900° C where fairly rapid reduction will occur with minimum sintering of the product. From the EDAX analysis of the various powder products it is apparent that a small amount of segregation has occurred (as a result of tungsten precipitation and the formation of the amorphous phase); however this segregation does not seem to be on a large enough scale to cause problems in the production of WC–Co composite powders by subsequent carburization.

## 5. Conclusions

1. The reduction of various $CoWO_4$-based oxide mixtures at temperatures of the order of 600 to 900° C does not give the equilibrium products which may be predicted from the appropriate section of the W–Co–O phase diagram.

2. The reduction process proceeds via the formation of an amorphous phase which retains all the cobalt until fairly advanced stages in the reduction process (typically 53 to 70% reduction).

3. The amorphous phase becomes enriched with cobalt as either metallic tungsten (for cobalt-rich oxide mixtures) or as $WO_2$ (for tungsten-rich oxide mixtures) are produced during the early stages of reduction. The amorphous phase becomes unstable at a critically low oxygen potential (below the equilibrium value for $WO_2$) during the later stages of reduction.

4. The degree of enrichment of the ternary amorphous phase, which depends upon the temperature and rate of reduction, dictates which cobalt-containing intermetallic compound is produced as reduction nears completion. At low temperatures $Co_3W$ is produced (600° C) whereas at higher temperatures the amount of $Co_3W$ decreases as the amount of $Co_7W_6$ increases. At temperatures greater than 800° C (for tungsten-rich mixtures) and 900° C (for cobalt-rich mixtures) $Co_7W_6$ and α-tungsten are the only reaction products identified by X-ray diffraction analysis.

## Acknowledgements

The authors would like to thank SERC and Murex Ltd, for funds and materials which have allowed this study to be carried out as part of an SERC CASE award project.

## References

1. F. GORTSEMA and P. KOTVAL, *Plansee. Pulvermet.* **24** (1976) 254.
2. S. TAKATSU, *Powder Met. Int.* **10** (1978) 13.
3. K. USHIJIMA, *ibid.* 11 (1979) 158.
4. T. D. HALLIDAY, F. H. HAYES and F. R. SALE in "Industrial Uses of Thermochemical Data", edited by T. I. Barry, Special Publication No. 34 (Chemical Society, London, 1980) p. 291.
5. G. J. FRENCH, PhD thesis, University of Manchester (1983).
6. J. GUERASSIMOV, Proceedings 16th IUPAC International Congreess of Pure and Applied Chemistry, Paris (Butterworth, London, 1957) p. 227.
7. A. K. BASU and F. R. SALE, *J. Mater. Sci.* **12** (1977) 1115.
8. *Idem, ibid.* **13** (1978) 2703.
9. P. WALKDEN and F. R. SALE, "Proceedings 2nd European Symposium on Thermal Analysis (ESTA-2)", Aberdeen (1981), edited by D. Dollimore (Heyden, London 1981) p. 531.
10. *Idem*, in "Electrical Contacts 1982", Proceedings 28th Annual Holm Conference on Electrical Contacts, Illinois Institute of Technology, Chicago (1982) p. 101.
11. P. BRACCONI and L. DUFOUR, *Met. Trans. B* **7B** (1976) 321.
12. *Idem, ibid.* **7B** (1976) 329.
13. T. EKSTROM and R. J. D. TILLEY, *J. Solid State Chem.* **22** (1977) 331.
14. N. SCHONBERG, *Acta Chem. Scand.* **8** (1954) 630.
15. W. MORCOM, W. WORRELL, H. SELL and H. KAPLAN, *Met. Trans.* **5** (1974) 155.
16. A. K. BASU and F. R. SALE, in "Modern Developments in Powder Metallurgy", Vol. 9,

edited by H. H. Hausner and P. V. Taubenblat, (Metal Powder Industries Federation and American Powder Metallurgy Institute, New Jersey, 1977), p. 171.

17. T. WILKEN, C. WERT, J. WOODHOUSE and W. MORCOM, *ibid*., p. 161.

*Received 9 May*
*and accepted 1 June 1984*